

# Observational evidence for the Ekman layer

## lecture by Steve Lentz

Lecture 4 by Miranda Holmes

This lecture focusses on observations that test the Ekman dynamics developed so far and to come.

**Eddy viscosity** Recalling that the size of the Ekman layer is  $\delta_E = \sqrt{2\nu/f}$  and using typical values of  $\nu = 10^{-6}m^2/s$ ,  $f = 10^{-4}s^{-1}$  gives  $\delta_E = 10cm$ . However, in the ocean  $\delta_E$  is on the order of 10m, suggesting that we should use a much higher viscosity coefficient of  $\nu^{\text{ocean}} = 10^{-2}m^2/s$ . This can be achieved by a suitable parameterization of an eddy viscosity.

We define a turbulent eddy-viscosity coefficient  $A$  such that

$$Au_z \approx -\langle u'w' \rangle .$$

Unlike the molecular viscosity  $\nu$ ,  $A$  depends on the flow and the stratification.

Madsen ([Madsen \(1977\)](#)) found that a suitable form for  $A$  in a turbulent Ekman layer is

$$A = \kappa u_* z , \quad u_* = \sqrt{\tau^s/\rho_0} , \quad (1)$$

where  $z$  is the distance from the boundary,  $\tau^s$  is the applied stress, and  $\kappa = 0.4$  is Von Karman's constant. This form can also be derived through dimensional arguments. If we define  $u_* = \sqrt{\tau^s/\rho_0}$ , then the stress at the surface is  $\tau^s/\rho_0 = Au_* z$ . From dimensional analysis, we have that  $uz \propto u_* z$ . Letting the constant of proportionality be  $1/\kappa$  gives (1).

This is the parametrization most often used to test Ekman theory. It can be used to derive the frequently-cited Law of the Wall. Integrating  $uz = \frac{1}{\kappa} \frac{u_*}{z}$  gives the Law of the Wall:

$$\sqrt{u^2 + v^2} = \frac{u_*}{\kappa} \ln(z) - \frac{u_*}{\kappa} \ln(z_0) , \quad u_* = \tau^b/\rho_0 \quad (2)$$

**Reminder Ekman Dynamics** Recall that in a steady wind-driven flow with no horizontal variations in the flow field or density field, the Ekman transport is

$$\int_{-\infty}^0 (v - v^g) dz = 0 \quad \int_{-\infty}^0 (u - u^g) dz = \frac{\tau_y^s}{\rho_0 f} ,$$

where  $\tau_y^s$  is the  $y$ -component of the surface stress. (The  $x$ -component is assumed to be 0.) (Note that the roles of  $u$  and  $v$  have been interchanged from the previous lectures.) This depth-integrated result is independent of the vertical viscosity, provided there is a depth where the internal stress is small compared to the surface stress. This feature allows us to test the Ekman transport predictions even though we don't have a full understanding of the details of the mixing processes.

**Testing the Theory** To test the theory, we need the following:

1. Velocity profiles ( $u(z), v(z)$ ) to sufficient accuracy and vertical resolution.
2. Surface stress  $\tau^s$ . This is typically found from a bulk formula using wind velocity measurements.
3. Geostrophic velocity, or a way to determine where  $\tau = 0$ , to separate the boundary layer from the interior flow.
4. Filtering out of high frequency ( $1/f$ ) velocity variability, since we usually neglect accelerations in the calculation of the Ekman transport.

**Observational Tests of the Ekman Transport Relationship** The following two studies have been important in verifying the Ekman transport relationship:

- Price, Weller, Schudlich, Science 1987
- Chereskin, JGR 1995

Both took measurements for about 160 days, and integrated down to a boundary layer thickness of about 50m. The plots of measured average transport, compared to theoretical Ekman transport, show excellent agreement (see figures 1, 2).

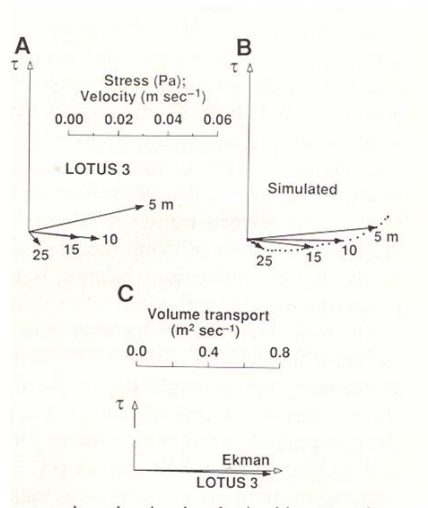


Figure 1: Observed and simulated Ekman spiral (A,B). Measured transport versus theoretical transport (C). (Price and Schudlich (1987))

They also showed the qualitative characteristics of the Ekman spiral, with the mean velocity turning to the right (in the northern hemisphere) and decreasing as depth increases. (Figures 1, 2).

**Observations of the Ekman spiral under ice** Hunkins (K.Hunkins (1966)) dropped a drogue under ice and measured the drag on it. The drag was used in a force balance to infer the velocity. From this, he obtained a picture of an Ekman spiral below the ice (Figure 3).

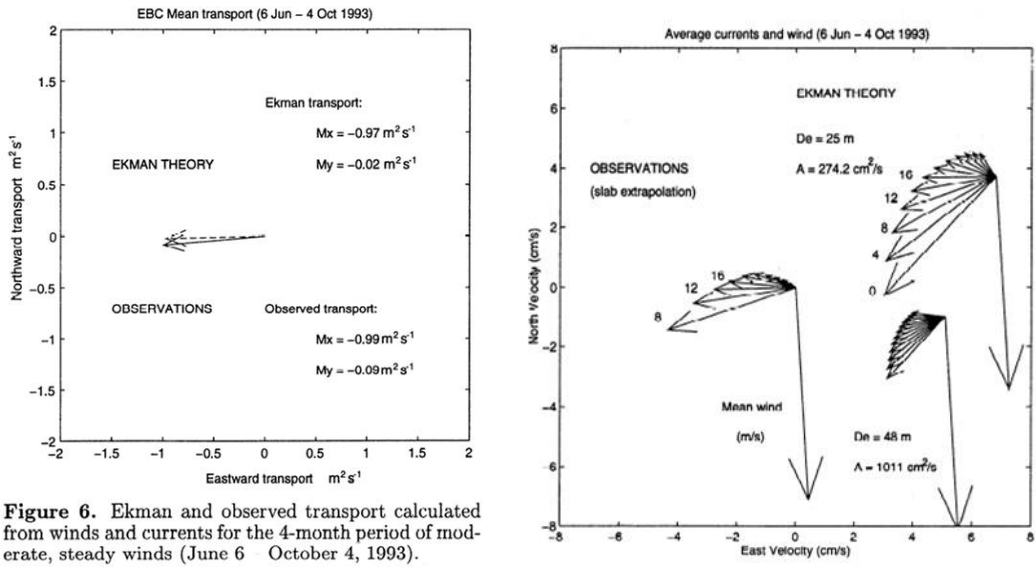


Figure 6. Ekman and observed transport calculated from winds and currents for the 4-month period of moderate, steady winds (June 6 - October 4, 1993).

Figure 2: (Chereskin (1995))

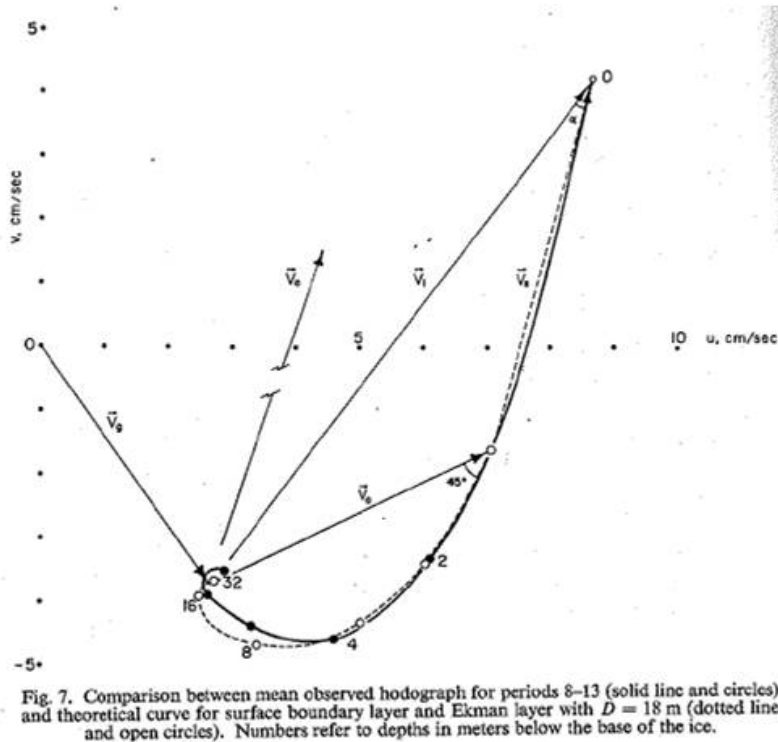


Figure 3: (K.Hunkins (1966))

**Surface Mixed Layer** Lentz (Lentz (1992)) measured the depth of the mixed layer and compared it to the wind stress and the depth of the wind-driven flow. He found there was a good correlation between the wind stress and the depth of the mixed layer. The depth of the wind-driven flow also depended on the wind stress, but tended to exceed the mixed-layer depth.

**Summary of surface Ekman layer** There is convincing evidence of wind-driven transport with the right magnitude and direction, which extends beyond the mixed layer. Note that it is only the *mean* profiles that veer clockwise - the profiles at any instant of time show large fluctuations on storm timescales (1 day) and diurnal timescales. Present research is focused on (a) the character of turbulent mixing in the boundary layer; and (b) the role of surface waves in determining the vertical structure of the flow - these have the additional complication of introducing a non-rigid boundary and wave momentum transfer.

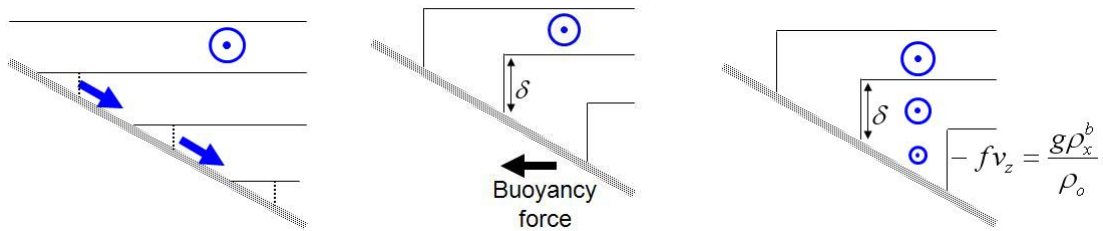


Figure 4: A bottom that is sloping with respect to the isopycnals introduces a buoyancy force in the boundary layer that may be important to the dynamics.

**Bottom boundary layer** Ekman theory is essentially the same if the bottom is flat, or if the flow is unstratified and the slope is small. However, for stratified flow over a sloping bottom, a buoyancy force comes into play that may dominate the dynamics. Here we give a brief, qualitative description of this buoyancy force - it will be described with more rigor in the next lecture.

Suppose we have a stably stratified flow along a bottom of slope  $\alpha$ . Stress on the bottom results in vertical mixing and up- or down-slope Ekman transport (figure 4 left). This flow displaces the isopycnals, and a buoyancy force develops that may oppose the interior pressure gradient (figure 4 center). This buoyancy force reduces  $v$  in the bottom boundary layer through the thermal wind balance,  $-fv_z = g\rho_x^b/\rho_o$ , so the stress on the bottom is reduced. As the boundary layer continues to grow,  $v$  decreases at the bottom (figure 4 right). Eventually a steady-state is reached where the bottom stress, and hence the Ekman transport, are both zero, so the isopycnals are displaced no further. At the bottom, the pressure gradient of the interior flow is balanced by the buoyancy force in the boundary layer. The end result is geostrophic flow that just happens to be zero at the bottom.

If the flow is out of the page and the slope is as in Figure 5, then the Ekman transport is initially down the slope. This advects light fluid under heavy, creating convective instabilities, which enhance mixing, so we expect a thicker boundary layer. If the flow is into the page, then the Ekman transport is initially upslope, advecting heavy fluid under lighter, so we expect a thinner boundary layer because this configuration is convectively stable.

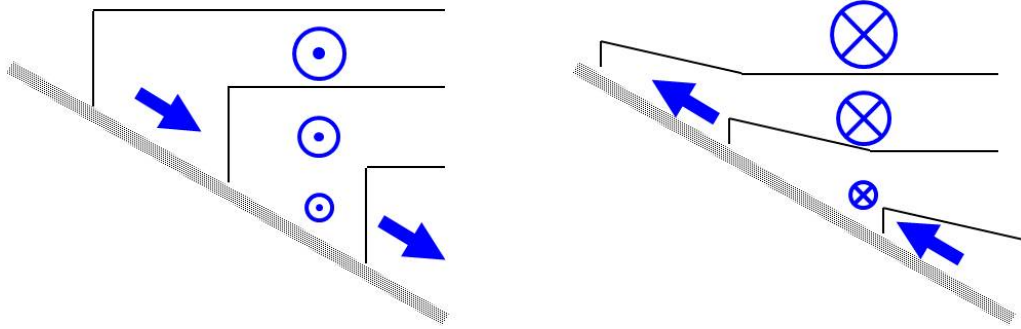


Figure 5: Downslope Ekman transport produces a thick boundary layer (left), while upslope Ekman transport produces a thinner layer (right).

**Observations of the bottom boundary layer** There are relatively few observational studies of the bottom boundary layer. References (Weatherly and Martin (1978)), (Trowbridge and Lentz (1991)), (MacCready and Rhines (1991)), (MacCready and Rhines (1993)), (Garrett and Rhines (1993)) are some of the main ones. Here we summarize results from a small number of studies.

Lentz and Trowbridge (Lentz and Trowbridge (1991)) tested the hypothesis that the thickness of the boundary layer across a sloping bottom should depend on the direction of the flow, using data taken from the Northern California shelf. Because of the turbulence created by the strong shear near the sea floor, the bottom boundary layer tends to be well-mixed, with nearly homogeneous temperature and density profiles. This allowed them to characterize the height of the bottom boundary layer as the place where the temperature deviated from the temperature at the sea floor by more than a given amount. In their experiment, they characterized the height of the boundary layer as the place where  $|T - T_b| < 0.05^\circ\text{C}$ . They found a good correlation between the direction of the flow and the thickness of the boundary layer. Figure 6 (left) shows that the estimated boundary layer height is larger when the flow is downwelling, and smaller when the flow is upwelling. Figure 6 (right) plots this correlation.

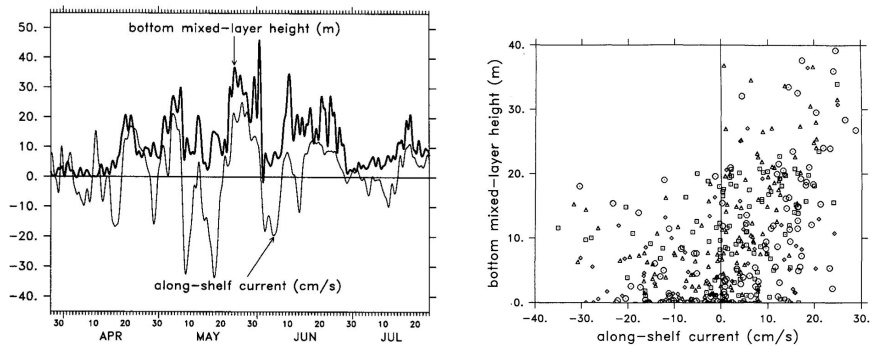


Figure 6: Left: The thickness of the bottom boundary layer (the bottom mixed-layer height) is greater when the along-shelf current is positive, inducing a downwelling Ekman flux, than when it is negative, with an induced upwelling flux. Right: Bottom mixed-layer height versus along-shelf current. (Lentz and Trowbridge (1991))

Moum et al (Moum and Kosro (2004)) looked for convectively driven mixing in the bottom boundary layer, which should be present if the flow is downwelling. Their measurements showed an unstable density gradient near the bottom, typical of convection. The slope was in good agreement with the Law of the Wall scaling (equation (2)).

Many previous observational studies have noted a qualitative ‘Ekman-like’ veering of the velocity field near the bottom. However, this needs to be looked at more quantitatively. Two questions of interest are: (1) Does the Ekman balance hold? (2) If not, are the cross-isobath buoyancy forces significant in the cross-isobath momentum balance? The bottom boundary layer momentum balance has been tested in two observational studies.

Trowbridge and Lentz (Trowbridge and Lentz (1998)) looked at 2 years of data off the Northern California shelf. They measured the transport with current meters, and estimated the stress using the Law of the Wall (2). The buoyancy force was estimated from temperature measurements. As in other studies, the boundary layer was defined to be the place where  $|T - T_b| < 0.05$ .

Because they had the appropriate data, they included acceleration terms in their calculations of the terms in the momentum balances. The equations they used are

$$\begin{aligned} \rho_0 \int_0^\delta [ut - (ut)_\delta] dz - \underbrace{\rho_0 f \int_0^\delta (v - v_\delta) dz}_{\text{Ekman transport}} &= \underbrace{\beta g \left[ \frac{\delta^2}{2} T_x + \alpha \int_0^\delta (T - T_\delta) dz \right]}_{\text{buoyancy force}} - \tau_x^b \\ \rho_0 \int_0^\delta [vt - (vt)_\delta] dz + \underbrace{\rho_0 f \int_0^\delta (u - u_\delta) dz}_{\text{Ekman transport}} &= \underbrace{\beta g \frac{\delta^2}{2} T_y}_{\text{buoyancy force}} - \tau_y^b \end{aligned}$$

If they neglected the buoyancy term, they found a poor agreement between the wind stress and Ekman transport (Figure 7 top), particularly during large boundary layer transport events. If the buoyancy force was included, the agreement was better (Figure 7 middle), showing that the buoyancy term is as large as the bottom stress, particularly during downwelling when the bottom mixed layer is thick.

Perlin et al (Perlin and Klymak (2005)) looked at the momentum balance in transects of the Oregon shelf. They measured the cross-shelf bottom boundary layer velocity  $u_b$  and compared it to the Ekman velocity estimated from Ekman balance:  $u_{EK} = \frac{\tau^{by}}{\rho_0 f \delta E}$ . Although they neglected the buoyancy force, they found a good agreement between these velocities in the moored observations (Figure 8)

These two studies show that the current observational evidence supporting either Ekman balance, or the importance of the buoyancy force in the bottom boundary layer, is very limited.

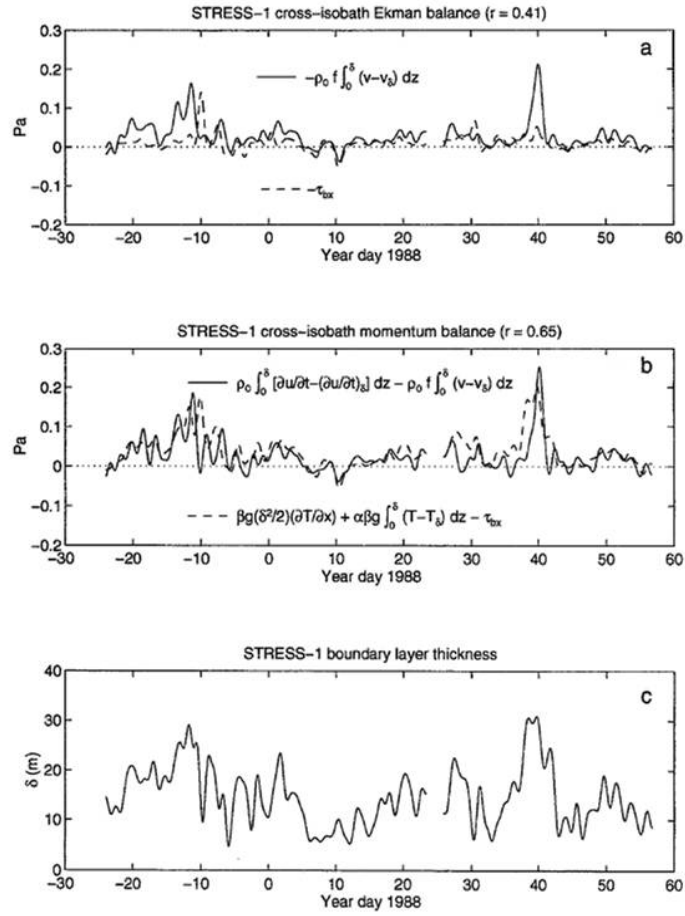
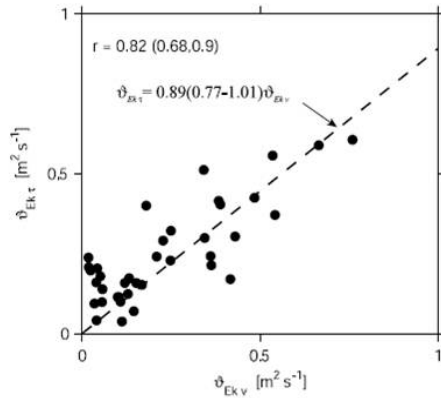


Figure 7: Wind stress (dotted) and Ekman transport (solid), neglecting the buoyancy term (top) and including the buoyancy term (middle) (Trowbridge and Lentz (1998))



**Figure 14.** Comparison of the transport computed by vertical integration of the velocity perpendicular to that at height  $D_{Ek}$  using moored velocity data (3 month time series), and the Ekman transport computed from bottom stress using a drag coefficient and the current speed at 20 m.

Figure 8: (Perlin and Klymak (2005))

## References

- T. K. Chereskin. Direct evidence for an ekman balance in the california current. *J. Geophys. Res.*, 13:18,261–18,269, 1995.
- P. MacCready Garrett, C. and P. Rhines. Boundary mixing and arrested ekman layers: rotating stratified flow near a sloping boundary. *Ann. Rev. Fluid Mech.*, 25:291–323, 1993.
- K.Hunkins. Ekman drift currents in the arctic ocean. *Deep Sea Res.*, 13:607–620, 1966.
- S. J. Lentz. The surface boundary layer in coastal upwelling regions. *J. Phys. Oceanogr.*, 22: 1517–1539, 1992.
- S. J. Lentz and J. H. Trowbridge. The bottom boundary layer over the northern california shelf. *J. Phys. Oceanogr.*, 21:1186–1201, 1991.
- P. MacCready and P. B. Rhines. Buoyant inhibition of ekman transport on a slope and its effect on stratified spin-up. *J. Fluid Mech.*, 223:631–661, 1991.
- P. MacCready and P. B. Rhines. Slippery bottom boundary layers on a slope. *J. Phys. Oceanogr.*, 23:5–22, 1993.
- O. S. Madsen. A realistic model of the wind-induced ekman boundary layer. *J. Phys. Oceanogr.*, 7:248–255, 1977.
- A. Perlin J. M. Klymak M. D. Levine T. Boyd Moum, J. N. and P. M. Kosro. Convectively driven mixing in the bottom boundary layer. *J. Phys. Oceanogr.*, 34:2189–2202, 2004.

- J. N. Moum, Perlin, A. and J. M. Klymak. Response of the bottom boundary layer over a sloping shelf to variations in alongshore wind. *J. Geophys. Res.*, 110:C10S09,doi:10.1029/2004JC002,500, 2005.
- R. A. Weller, Price, J. F. and R. R. Schudlich. Wind-driven ocean currents and Ekman transport. *Science*, 238:1534–1538, 1987.
- J. H. Trowbridge and S. J. Lentz. Asymmetric behavior of an oceanic boundary layer above a sloping bottom. *J. Phys. Oceanogr.*, 21:1171–1185, 1991.
- J. H. Trowbridge and S. J. Lentz. Dynamics of the bottom boundary layer on the northern California shelf. *J. Phys. Oceanogr.*, 28:2075–2093, 1998.
- G. L. Weatherly and P. J. Martin. On the structure and dynamics of the oceanic bottom boundary layer. *J. Phys. Oceanogr.*, 8:557–570, 1978.